

PRECISION MEASUREMENTS OF THE THERMAL CONDUCTIVITY,  
ELECTRICAL RESISTIVITY, AND SEEBECK COEFFICIENT  
FROM 80 TO 400 K AND THEIR APPLICATION TO PURE MOLYBDENUM\*

J. P. Moore, R. K. Williams, and R. S. Graves  
Metals and Ceramics Division  
Oak Ridge National Laboratory  
Oak Ridge, Tennessee 37830

ABSTRACT

A longitudinal heat flow technique for precise measurement of thermal conductivity, electrical resistivity, and Seebeck coefficient over the temperature range from 80 to 400 K is described. The basis of the technique is the use of a calibrated platinum resistance thermometer to provide in situ calibrations of specimen thermocouples. The total determinate errors at 273 K are  $\pm 0.23\%$  for electrical resistivity,  $\pm 0.49\%$  for thermal conductivity, and  $\pm 0.07 \mu\text{v/K}$  for the Seebeck coefficient when Pt wire is used as the reference. Experimental results on two high-purity molybdenum specimens with cross-sectional areas differing by a factor of four are presented to demonstrate the system precision and low level of indeterminate errors.

INTRODUCTION

There have been numerous thermal conductivity,  $\lambda$ , measurements made with longitudinal heat flow systems. Longitudinal systems built for operation below 50 K have been operated successfully in vacuo both without thermal guards and without insulation between specimen and guard because radiation transfer is negligibly small at low temperatures. Above 50 K, however, guard tubes and thermal insulation between specimen and guard are essential

---

\*Research sponsored by the U. S. Atomic Energy Commission under contract with the Union Carbide Corporation.

**MASTER**

to insure linear heat flow; and above about 300 K (depending on the ratio of conductivities of the specimen and the insulation), corrections for radial heat flow in the specimen and hence across the specimen-guard annulus are necessary to reduce  $\lambda$  measurement uncertainties to one or two percent.<sup>(1)</sup> The authors have previously described<sup>(2)</sup> a guarded longitudinal device for measurements of  $\lambda$ , the absolute Seebeck coefficient,  $S$ , and electrical resistivity,  $\rho$ , over the  $T$  range from 80 to 400 K. This older device has been employed on a wide variety of materials<sup>(3-4)</sup> with modifications in the details for different applications. It had a most probable determinate error for  $\lambda$  measurements of  $\pm 1.2\%$  and comparison to other techniques<sup>(5)</sup> using common or companion samples indicated that the absolute accuracy was also about  $\pm 1\%$ .

To enhance studies of  $\rho$  and  $\lambda$  in pure metals and dilute alloy systems,<sup>(6)</sup> it was necessary to further reduce measurement uncertainties in  $\rho$  and  $\lambda$ ; and the attempt to do so is described herein. Laubitz and McElroy<sup>(5)</sup> should be studied for a complete description of the problems involved in making precise  $\lambda$  measurements.

The largest source of error in the older  $\lambda$  technique was determination of the temperature gradient along the specimen and this has been reduced by an in situ calibration of specimen thermocouples against a platinum resistance thermometer (PRT). This is not the first attempt to perform an in situ thermocouple calibration in this  $T$  range since Slack et al.<sup>(7)</sup> used a gas bulb thermometer and Cook et al.<sup>(8)</sup> also used a PRT. The  $S$  and  $\lambda$  measurements are both dependent on the temperature gradient; and since  $S$  can be determined using both Pt wire and constantan wire, the two determinations of  $S$  can serve as internal checks of system precision.

-NOTICE-

This report was prepared as an account of work sponsored by the United States Government. Neither the United States nor the United States Atomic Energy Commission, nor any of their employees, nor any of their contractors, subcontractors, or their employees, makes any warranty, express or implied, or assumes any legal liability or responsibility for the accuracy, completeness or usefulness of any information, apparatus, product or process disclosed, or represents that its use would not infringe privately owned rights.

Many errors in longitudinal systems are proportional to the thermal resistance of the specimen. To assist in assessing these, measurements of  $\lambda$ ,  $\rho$ , and  $S$  have been made on two high purity Mo samples with cross-sectional areas differing by a factor of about four. Results from the two samples are compared and suggestions for possible further reductions of errors are made.

#### TECHNIQUE DESCRIPTION

The sample chamber of the apparatus is shown in Fig. 1 and Fig. 6 of Ref. 5 shows the earlier version. As in the predecessor, the specimen is mounted inside a vacuum chamber with one end of the specimen secured in a Cu holder and a heater  $H_1$  on the free end. Two Chromel-P versus constantan thermocouples and two platinum wires were welded to the specimen at known positions. All of these wires were attached far enough from the Cu holder and heater  $H_1$  to negate end effects and insure that  $dT/dr$  and  $dT/d\theta$  were approximately zero, where  $T$  was the temperature and  $r$  and  $\theta$  the cylindrical coordinates. The shortest distance between the thermocouples and  $H_1$  or the Cu holder was one specimen diameter. This distance was selected after a study of end effects in electrical potential drop measurements. Heater wires from  $H_1$  passed through a thermal ground point on the guard cylinder and thermocouples were used to determine the temperatures of  $H_1$  and of the thermal ground. Heater  $H_2$  was employed to raise the thermal ground temperature until it was equal to  $T$  of  $H_1$ . Heater  $H_3$  was used to control the ambient temperature of any measurement above the bath which was either of ice-water or liquid nitrogen. The annulus between specimen and guard cylinder was filled with a spun-fibrous insulation<sup>(9)</sup> of low thermal conductivity.<sup>(10)</sup>

There were three primary differences between the older and the present design. First, a Cu sleeve was added on the main guard cylinder where  $H_2$

was attached and where the thermal ground was made. This was done to insure that the region around the thermal ground was isothermal. Secondly, a platinum resistance thermometer (PRT) was attached to the specimen base to permit in situ calibration of the thermocouples. Lastly, all thermocouple wires and the 2 Pt wires were attached to the lead in wire (of the same material) at connections which were designed to maintain the wire junctions near the bath T but electrically insulated from the metal flange. This thermal anchoring of the junctions was necessary for suppressing time varying thermal emfs at these connections.

A schematic of the system is shown in Fig. 2. The specimen heater  $H_1$  was powered with a stabilized D.C. power supply<sup>(11)</sup> with the current passing through a 0.1 ohm standard resistor<sup>(12)</sup> and a reversing switch. The voltage drop across the standard resistor was determined using a Guildline Model 9930 Potentiometer<sup>(13)</sup> (henceforth called the GP). The potential drop across  $H_1$  was determined using a Leeds and Northrup<sup>(14)</sup> K-5 potentiometer and a voltage divider<sup>(15)</sup> to reduce the voltage across  $H_1$  to the potentiometer level. Thermocouples #1 on  $H_1$  and #2 on  $H_2$  were differentially connected and the difference fed to a controller which adjusted power in  $H_2$ . This controller was capable of matching the temperatures at  $H_1$  and  $H_2$  to within  $\pm 0.02$  degrees. Heater  $H_3$  consisted of an insulated nichrome wire wound on either a brass or copper rod depending on the coolant and the desired operation temperature. The voltage to this heater was automatically controlled to maintain the temperature of the system stable to about  $\pm 0.004$  K. All heaters ( $H_1$ ,  $H_2$ , and  $H_3$ ) were wound directly onto the metal surfaces and bonded into place with thermally conducting epoxy<sup>(16)</sup> to minimize temperature differences between heater wires and surfaces.

Platinum wires on the specimen were referenced to the ice point and their EMF determined with the K-5 whereas the Chromel-P versus constantan thermocouples on the specimen were referenced to the ice point and passed through a selector switch<sup>(17)</sup> to the GP for EMF determination. The Cu wire between the reference ice bath and the GP was low thermal, electrostatically shielded cable.<sup>(18)</sup> Copper wires and switching circuits to the K-5 were similar to those described by Godfrey *et al.*<sup>(19)</sup>

The PRT current was supplied by a battery and passed through a reversing switch and a 10 ohm standard resistor.<sup>(20)</sup> Voltage drops across the PRT and standard resistor were measured with the GP.

#### Platinum Resistance Thermometer

The He filled PRT<sup>(21)</sup> used for in situ thermocouple calibrations was 1.27 cm long and 0.32 cm diam. This type of thermometer was the subject of a recent stability and calibration test by Johnston and Lindberg<sup>(22)</sup> which confirmed their usefulness over the T range of interest.

As shown in Fig. 3, the PRT was bonded into a slip fit hole in a Cu plate using thermally conducting epoxy.<sup>(16)</sup> The four Pt wires from the PRT were thermally grounded with epoxy on the Cu plate to prevent heat loss from the PRT element. The Cu plate was attached to the specimen base with machine screws with a sheet of In foil (0.012 cm thick) compressed between the Cu surfaces to reduce interfacial resistance. Before installation the PRT was calibrated on the IPTS-68 scale<sup>(23)</sup> from 78 to 423 K and subsequent care was taken to prevent temperature excursions beyond those limits.

#### Ice Bath References

A special ice bath was constructed to reference all thermocouples and Pt wire used for S measurements to the ice point. This bath was designed to provide adequate immersion depth for all wires.<sup>(24)</sup> The design of the ice bath reference was similar to the unit employed with the original  $\lambda$

apparatus and described by Kollie.<sup>(25)</sup> The one major change involved positioning the reference junctions of the two specimen thermocouples in a single well. This well consisted of an annular mineral oil filled space with copper walls. During operation, the ice bath was replenished every few hours to prevent excessive water collection in the dewar bottom.

The ice used in the bath was made from normal, undistilled, tap water which had enough minerals present to depress the freezing point by 0.005 K. Routine checks of the dissolved chemicals in the tap water indicated that they varied little with time and that the electrical resistivity was approximately  $50 \times 10^3$  ohm-cm. The slight lowering of the ice bath temperature below the ice point had no effect on this experiment since the thermocouples were calibrated against the PRT which was not directly based on a bath reference temperature.

#### Thermal Ground on the Guard Cylinder

To minimize extraneous heat flow to or from  $H_1$ , the copper heater wires from heater  $H_1$ , the thermocouple wires from T.C. #1, and the  $\rho$  current lead to the top of the specimen were thermally grounded on the guard cylinder. The temperature of this ground was accurately determined and care taken not to electrically short the insulation of the  $H_1$  wires at this position. To accomplish this the enameled Cu wires from  $H_1$  were spiraled around the two fiberglass insulated thermocouple wires as shown in Fig. 4. A blanket of indium foil (0.025 cm thick) was placed around the region which had the spiraled Cu wire. Thermocouple #2 was placed on top of the In blanket and a flexible metal clamp compressed the assembly. Under pressure from the clamp, the In flowed around the Cu wires and placed the wires in thermal contact with the Cu part of the guard cylinder and the thermocouple without cutting through the insulating enamel on the Cu wire.

Potential taps for determining the voltage drop across  $H_1$  were placed outside the thermal ground and this necessitated a small correction which will be described in a later section.

#### OPERATION

Operation of the earlier version of this technique required that all temperatures be determined during steady state conditions for two temperature distributions. <sup>(2,5)</sup> The first distribution was the "isothermal" and was essentially an intercomparison of specimen thermocouples when the power dissipated in  $H_1$  was zero and thermocouples #1 and #2 were matched in T to prevent heat flow along wires between  $H_1$  and the guard cylinder thermal ground. For the second distribution, heater  $H_1$  was energized with a D.C. voltage to establish a 5 to 7 degree  $\delta T$  between specimen thermocouples and the average specimen temperature was adjusted to the same value for the "isothermal" using heater  $H_3$ . The measured power dissipated in  $H_1$  and the measured  $\delta T$  as corrected for the isothermal intercomparison were used to calculate  $\lambda$ . This approach assumed a previous calibration for the T.C. wires, and the isothermal was used to correct for small T.C. differences introduced during assembly and for small extraneous heat flow. <sup>(5)</sup>

In the present technique, the Chromel-P versus constantan thermocouples were individually calibrated in situ against the PRT during the isothermal test by assuming that the measuring junctions on the specimen were at the same T as the PRT. The EMF, E, from each T.C. was then fit to

$$E = A_1 + B_1(T-273.15) + C_1(T-273.15)^2 + D_1(T-273.15)^3 \quad (273 < T < 410) \quad (1)$$

when the chamber was cooled with an ice bath and

$$E = A_2 + B_2(T-273.15) + C_2(T-273.15)^2 + D_2(T-273.15)^3 + E_2(T-273.15)^4 \quad (73 < T < 300) \quad (2)$$

when the coolant was liquid nitrogen. The EMFs from Chromel-P versus constantan thermocouples fit Eq. (1) (less the constant term) from 273 to 423 K and Eq. (2) from 73 to 273 K to within  $\pm 0.4 \mu\text{v}$  as can be shown by fits to smoothed tables.<sup>(26)</sup> The constant terms in Eqs. (1) and (2) are necessary to account for small thermals in the thermocouple circuits especially at junctions; and with the constant term included, the above equations fit our calibration data to within  $\pm 0.2 \mu\text{v}$  ( $\pm 0.008$  degrees at 80 K and  $\pm 0.003$  degrees at 400 K).

After completing a series of isothermals to calibrate each specimen T.C. in ice-water or nitrogen baths, a gradient was established along the specimen using  $H_1$ . The base heater  $H_3$  was used to maintain the system at the desired T and heater  $H_2$  was used to match the temperatures indicated by T.C. 1 and T.C. 2. Heater  $H_3$  and its associated control circuitry maintained the output of the control T.C. constant to within  $\pm 0.1 \mu\text{v}$  ( $\pm 0.004$  K at 80 K and  $\pm 0.0015$  K at 400 K). The small temperature oscillations at the control T.C. were damped by the thermal mass between  $H_3$  and the specimen so that during any given test T of the specimen varied by  $< \pm 0.004$  K. After the specimen reached steady state with a short term drift rate  $< 0.0002$  deg/min, the EMFs from all the thermocouples, the constantan and Chromel-P thermoelements of the specimen thermocouples and the Pt wires were measured. In addition, the voltage drop across  $H_1$  and the current through  $H_1$  were measured. The heat conducted down the specimen was calculated from the measured electrical power,  $P_e$ , dissipated in  $H_1$ . This measured power was corrected for several small effects which include voltage divider calibration (0.01%), current shunting through the voltage divider (0.02%) and potential tap placement. The potential tap corrections were necessary since the voltage measuring points were outside the thermal ground. Since Cu wire was used for current leads to  $H_1$ , the latter correction was proportional

to  $\rho$  of Cu which varies with T so that this correction was  $-0.02\%$  at 80 K and increased to  $-0.18\%$  at 400 K.

The EMF values from the two Chromel-P versus constantan thermocouples on the specimen were converted to temperature using the appropriate parameters for equations (1) and (2). The EMFs between constantan wires of the specimen thermocouples and between Pt wires on the specimen were used for calculation of the Seebeck coefficient of Mo with respect to Pt,  $S_{\text{Mo-Pt}}$ , and with respect to constantan,  $S_{\text{Mo-Co}}$ . Absolute values for  $S_{\text{Pt}}$  and  $S_{\text{Co}}$  were obtained from Moore and Graves<sup>(4,27)</sup> for calculating  $S_{\text{Mo}}$ .

The electrical resistivity data were determined using a standard 4 probe D.C. technique with a current reversing switch. The voltage drop along the specimen was determined by reading the EMF between the Chromel-P thermoelements with the GP and the current was determined by measuring the voltage drop across a  $0.1 \Omega$  standard resistor using the K-5.

#### SPECIMEN DESCRIPTION

Characteristics of the two molybdenum specimens whose properties were investigated and compared are given in Table 1. For comparison purposes, it would be best if the two specimens differed only in size since that would remove any doubt about impurity differences. However, the best indicators of specimen purity are the residual electrical resistivity values ( $\rho_{4.2\text{K}}$ ); and the difference ( $0.0005 \mu\Omega\text{-cm}$ ) would indicate an expected difference in  $\rho$  of  $0.1\%$  at 80 K and  $0.01\%$  at 300 K. Specimen diameters were determined by two methods, the first involving direct measurements with calibrated micrometers. In the second method, the sample volume obtained during immersion density measurements was combined with the measured length to calculate the mean sample diameter. The diameter values quoted in Table 1 are the averages of the values obtained by the two methods which differed by  $0.04\%$  and  $0.02\%$  for A and B respectively. The distances between

Table 1. Characteristics of Molybdenum Specimens

	Specimen A	Specimen B
diam (cm)	0.3798	0.7721
density (g/cm <sup>3</sup> )	10.230	10.230
$\rho$ ratio ( $\rho_{300K}/\rho_{4.2}$ )	$8.0 \times 10^3$	$4.7 \times 10^3$
$\rho_{4.2K}$ ( $\mu\Omega\text{-cm}$ )	0.0007	0.0012
Vacuum Heat Treatment	2372 K for 1/2 hr 2173 K for 10 hrs	1873 K for 24 hrs

thermocouple wires and between Pt wires on the specimens were determined electrically by comparison of voltage drops to the voltage drop between knife edges of known spacing.

## MEASUREMENT UNCERTAINTIES

### Temperature Uncertainty

Since all three properties ( $S$ ,  $\rho$ ,  $\lambda$ ) are functions of  $T$ , it is appropriate that the uncertainty in this parameter be discussed first. Table 2 summarizes the error sources involved in determining the temperature during data tests and their magnitude. The calibration error of the PRT shown in the table was for 78 K where it was a maximum, but this value decreased to  $\pm 0.012$  degrees at 90 K,  $\pm 0.005$  degrees at 195 K and  $\pm 0.002$  degrees at the ice point. Errors number 2, 3 and 5 were due to uncertainties in standard resistors as well as potentiometer uncertainty in measuring the EMFs and error number 4 was calculated based on the scatter in the calibration of thermocouples against the PRT.

Error 6 was caused by temperature mismatch of T.C. #1 and T.C. #2 which caused heat to flow between the specimen and guard and hence generated a temperature difference between the specimen base, where the PRT was mounted, and the specimen thermocouples.

The maximum total determinate error of a calibrated thermocouple was thus  $\pm 0.038$  degrees and this occurred at 78 K. Because of the reduction in Error 1 with increasing  $T$ , the total determinate error was  $\pm 0.02$  degrees above 273 K.

There was one possible error in temperature measurement using the Chromel-P versus constantan thermocouples which could have been serious but was easily negated by care during assembly. The wire could have small thermal EMFs due to chemical inhomogeneities or wire strain.<sup>(28)</sup> If any spurious thermal EMF

Table 2. Errors in Temperature and Temperature Difference Determination  
by Thermocouples During Data Test

	Temperature Error (Degrees)	Error in $\delta T$ (%)
1. Calibration error of PRT	$\pm 0.02$	$\pm 0.015$
2. Resistance measurement of PRT	$\pm 0.007$	---
3. Potentiometer error in reading T.C. EMF during calibration	$\pm 0.0007$	---
4. Non-exact functional form of EMF (E) versus T	$\pm 0.008$	$\pm 0.23$
5. Potentiometer error in reading T.C. EMF during data	$\pm 0.0007$	$\pm 0.02$
6. Temperature of PRT and T.C. not equal during calibration due to extraneous heat flow along the specimen	$\pm 0.0003$	$\pm 0.01$
TOTAL	$\pm 0.038$ deg	$\pm 0.27$

changed between the calibration and the data T distribution, an error in T would have occurred. A shift of this type was most likely if the wire passed near a heater which changed T between calibration and data tests. For this reason, care was exercised to prevent wire passage near the tube which encloses heater  $H_3$ . Unnecessary wire strain due to bending was also avoided.

#### Uncertainty in the Temperature Difference

The temperature difference between the two specimen thermocouples was essential for calculating  $S_{Mo}$  and  $\lambda$  and the error involved in  $\delta T$  is shown in Table 2. Normally data were taken with a four to seven degree  $\delta T$  and errors in thermocouple calibration which occur gradually over a wide T range compared to the  $\delta T$  are not important. For example, suppose that the PRT calibration (Error 1 of Table 2) was off  $-0.02$  degrees at 80 K and  $+0.01$  degrees at 273.15 K. This would cause a relative error of 0.03 degrees in the calibration over a T range of nearly 200 degrees and an error of only 0.0010 degrees over a  $\delta T$  of 7 degrees if the calibration error were linear.

Errors 4 and 5 of Table 2 were, however, important and these lead to  $\delta T$  errors of  $\pm 0.23\%$  and  $\pm 0.02\%$ . Extraneous heat flow along the heater wires to  $H_1$  due to guard-specimen mismatch could have caused an error of  $\pm 0.01\%$  in  $\delta T$  and the total determinate error for the temperature difference was thus  $\pm 0.27\%$ , 85% of which was due to error 4.

#### Electrical Resistivity Uncertainties

The specimen  $\rho$  was calculated using

$$\rho = \frac{V_{\ell} R_{S.R.} A}{V_{S.R.} \ell} \quad (3)$$

where  $V_{\ell}$  is the voltage drop across a specimen length  $\ell$ ,  $V_{S.R.}$  the voltage drop across the standard resistance,  $R_{S.R.}$ , and  $A$  is the sample cross-sectional

area. The total determinate error in  $\rho$  would then be

$$\left| \frac{\Delta \rho}{\rho} \right| = \pm \left| \frac{\Delta V_{\ell}}{V_{\ell}} \right| \pm \left| \frac{\Delta V_{S.R.}}{V_{S.R.}} \right| \pm \left| \frac{\Delta R_{S.R.}}{R_{S.R.}} \right| \pm \left| \frac{\Delta \ell}{\ell} \right| \pm \left| \frac{\Delta A}{A} \right| \pm \left| \frac{d\rho}{dT} \frac{\Delta T}{\rho} \right| \quad (4)$$

where  $\Delta V_{\ell}$ ,  $\Delta \ell$ , etc., are the total uncertainties in  $V_{\ell}$ ,  $\ell$ , etc., and it has been assumed that  $\rho \propto T$  to give the last term. The uncertainties from various sources are given in Table 3 for the two Mo specimens described in an earlier section. Above 273 K the total determinate uncertainty would be  $\pm 0.34\%$  for specimen A and  $\pm 0.23\%$  for specimen B. Measurement imprecision would not involve the area and length uncertainties and this would indicate an expected imprecision of less than  $\pm 0.08\%$ .

#### Thermal Conductivity Measurement Uncertainties

The thermal conductivity was calculated from

$$\lambda = P_c \ell / A \delta T \quad (5)$$

where  $P_c$  is the power conducted down the specimen and  $\delta T$  is the temperature difference between the two thermocouples separated a distance  $\ell$ . The uncertainty in  $\lambda$  would thus be

$$\left| \frac{\Delta \lambda}{\lambda} \right| = \pm \left| \frac{\Delta P_c}{P_c} \right| \pm \left| \frac{\Delta \ell}{\ell} \right| \pm \left| \frac{\Delta A}{A} \right| \pm \left| \frac{\Delta(\delta T)}{\delta T} \right| \pm \left| \frac{d\lambda}{dT} \frac{\Delta T}{\lambda} \right| \quad (6)$$

where  $\lambda$  has been assumed directly proportional to  $T$  over small  $T$  intervals. The magnitudes of these errors are shown in Table 4 and all have been discussed except for the first and last.

Error in measurement of the electrical power dissipated in  $H_1$  was from several sources. Part of this was uncertainty in the potential tap placement which contributed  $\pm 0.007\%$  at 80 K and  $\pm 0.04\%$  at 273 K. In addition, potentiometer error, voltage divider error, and standard resistor error contributed  $\pm 0.03\%$ .

Most of the electrical power dissipated in  $H_1$  went down the specimen toward the heat sink, but some fraction of the heat flowed down the gradient

Table 3. Electrical Resistivity Uncertainties  
for Mo Specimens A and B

Source	Specimen A	Specimen B
$\frac{\Delta V_{\ell}}{V_{\ell}} + \frac{\Delta V_{S.R.}}{V_{S.R.}} + \frac{\Delta R_{S.R.}}{R_{S.R.}}$	$\pm 0.06\%$	$\pm 0.06\%$
$\frac{\Delta \ell}{\ell}$	$\pm 0.12\%$	$\pm 0.08\%$
$\frac{\Delta A}{A}$	$\pm 0.14\%$	$\pm 0.07\%$
$\frac{d\rho}{dT} \frac{\Delta T}{\rho}$	$\pm 0.13\%$ (80 K) $\pm 0.02\%$ (273 K)	$\pm 0.13\%$ (80 K) $\pm 0.02\%$ (273 K)
<b>Total Determinate</b>	$\pm 0.45$ (80 K) $\pm 0.34$ (273 K)	$\pm 0.34$ (80 K) $\pm 0.23$ (273 K)

Table 4. Thermal Conductivity Uncertainties  
for No Specimens A and B

Source	Specimen A	Specimen B
$\frac{\Delta l}{l}$	$\pm 0.12\%$	$\pm 0.08\%$
$\frac{\Delta A}{A}$	$\pm 0.14\%$	$\pm 0.07\%$
$\frac{\Delta(\delta T)}{\delta T}$	$\pm 0.27\%$	$\pm 0.27\%$
$\left(\frac{d\lambda}{dT}\right) \frac{\Delta T}{\lambda}$	$\pm 0.05\%$ (80 K) $\pm 0.00\%$ (273 K)	$\pm 0.05\%$ (80 K) $\pm 0.00\%$ (273 K)
$P_c$	$\pm 0.04\%$ (80 K) $\pm 0.07\%$ (273 K)	$\pm 0.04\%$ (80 K) $\pm 0.07\%$ (273 K)
<b>Total Determinate</b>	$\pm 0.62\%$ (80 K) $\pm 0.60\%$ (T > 273 K)	$\pm 0.51\%$ (80 K) $\pm 0.49\%$ (T > 273 K)

within the fibrous insulation and some may have flowed radially between specimen and guard cylinder depending on the temperature mismatch between the two. A mismatch problem was especially acute near  $H_1$  and  $H_2$  where it was virtually impossible experimentally to match temperatures at all values of  $z$ . For system flexibility and to minimize temperature drops between the heater wires and the surface to be heated, radially wound heaters were used for  $H_1$  and  $H_2$ , and this compounded the problem. Laubitz<sup>(1)</sup> has extensively investigated the temperature mismatch near this type heater for various ratios of specimen to insulation conductivity and concluded that the problem is severe enough that it might be better to match the specimen and guard gradients and then measure the power exiting the specimen at the cold end.

The temperature profile in the present system has been analyzed near 400 K for both specimens using a finite difference technique.<sup>(29)</sup> The problem model is shown in Figure 5 with all the dimensions for the smaller specimen (A) indicated. In addition to cylindrical symmetry, there were several assumptions made to simplify the calculations; and these include the following. The  $z = 0$  plane was located at the specimen junction with the Cu holder and this plane was assumed to be isothermal, interfacial resistances between regions such as  $H_1$  and the specimen were assumed to be negligible, and the match point of thermocouples #1 and #2 was at  $z = 6.23$  cm. Also, the brass section of the guard cylinder which had an actual thickness of  $r_4 - r_3$  was replaced with a material of thickness  $r_5 - r_3$  with a  $\lambda$  equal to one half that of brass.

All surfaces at  $r_5$  and the Al surface at  $z_7$  radiated heat out to the unheated guard furnace which was at a temperature two degrees below that of the  $z = 0$  plane. Most of the heat from  $H_2$  was conducted down the guard cylinder wall and this reduced the importance of assumed values for surface

emittances. The  $r$ - $z$  region covered by the system was divided into 405 lattice points. The computer calculated temperatures at each point for assumed power levels in  $H_1$  and  $H_2$ . The power in  $H_1$  was held constant and the power in  $H_2$  varied until the temperature at T.C. #1 and T.C. #2 were the same. Convergence criterion was between  $5 \times 10^{-8}$  and  $1 \times 10^{-7}$ . The results for calculations on specimen A are shown in the left side of Figure 6 where  $T$  is plotted for the inside wall of the guard cylinder [ $T(z, r_3)$ ], for the specimen surface from  $z = 0$  to 5.1 cm [ $T(z, r_1)$ ] and for the outer surface of  $H_1$  between  $z = 5.1$  and 7.27 cm [ $T(z, r_2)$ ]. Temperatures near the specimen centerline could have been shown but they were too near the outer surface temperatures to distinguish on the figure. The axial position where the two temperature profiles cross is at 6.23 cm where T.C. #1 and T.C. #2 were matched in  $T$  during the data distribution of the experiment. The  $T$  mismatch near this position was due to the Cu section of the guard cylinder since the thermal conductivity of the guard was so high that the guard becomes nearly isothermal with  $z$  whereas the surface of  $H_1$  does not.

The predecessor of this technique had a brass guard cylinder for all  $z$  values and the temperature distribution for that system is shown in Fig. 6 and is markedly better than the guard with a Cu section. Therefore, although the Cu section eliminated gradients in the vicinity of the thermal clamp, it exacted a price of increased specimen-guard mismatch and hence greater radial heat exchange.

Fortunately, the thermal conductivity of the fibrous insulation is low enough in vacuum<sup>(10)</sup> to make errors due to this mismatch low. The finite difference calculations discussed above indicate that radial exchange caused maximum  $\lambda$  effects of only +0.02% for specimen B and +0.06% for specimen A. These values were calculated for 400 K where they are a maximum since the

ratio of specimen to insulation conduction is lowest at that T. Values for heat flow through the fibrous insulation have been calculated versus T and applied as corrections to the measured  $P_e$  values.

Using previous values for the other error terms, the total determinate uncertainties for the two molybdenum specimens A and B are shown in Table 4 to be  $\pm 0.60\%$  and  $\pm 0.49\%$ , respectively, when  $T > 273$  K.

### Seebeck Coefficient Errors

The Seebeck coefficient was determined for specimen A using the constantan thermoelements of thermocouples three and four and for specimen B using both the constantan thermoelements and a pair of Pt wires attached at known positions. Errors in the Seebeck coefficient were different using the two type reference materials and were a function of T. Using the EMF from the Pt legs,  $S_{Mo}$  was calculated from the equation

$$S_{Mo} = S_{Mo-Pt} + S_{Pt} \quad (7)$$

or

$$S_{Mo} = \frac{E_{Pt}}{(\delta T)_{Pt}} + S_{Pt} \quad (8)$$

where  $S_{Mo}$  and  $S_{Pt}$  are absolute Seebeck coefficient values for Mo and Pt and  $S_{Mo-Pt}$  is the Seebeck coefficient of Mo with respect to Pt,  $E_{Pt}$  is the EMF between Pt thermoelements (as corrected for the small EMF obtained during the isothermal) and  $(\delta T)_{Pt}$  is the temperature drop between the wire attachment points along the specimen. This temperature drop is equal to a scale factor,  $\beta$ , times the temperature difference determined with thermocouples three and four so that

$$S_{Mo} = \frac{E_{Pt}}{\beta(\delta T)} + S_{Pt} \quad (9)$$

The errors due to determination of parameters in the above equation are shown in Table 5 and their sum shows that  $S_{Mo}$  would have a maximum determinate uncertainty of  $\pm 0.02 \mu\text{V/K}$  at 400 K.

Table 5. Seebeck Coefficient Determination Uncertainties at 400 K  
Using Pt and Constantan Thermoelements

Error Source	Error in $\mu\text{V}/\text{K}$	
	Pt	Co
E	$\pm 0.00$	$\pm 0.00$
$\beta$ or $\gamma$	$\pm 0.01$	$\pm 0.07$
$\delta T$	$\pm 0.05$	$\pm 0.15$
$S_{\text{Pt}}$ or $S_{\text{Co}}$	$\pm 0.02$	$\pm 0.17$
Max Determinate	$\pm 0.08 \mu\text{V}/\text{K}$	$\pm 0.39 \mu\text{V}/\text{K}$

Using the constantan thermoelements,

$$S_{Mo} = \frac{E_{Co}}{\gamma(\delta T)} + S_{Co} \quad (10)$$

where  $S_{Co}$  was the Seebeck coefficient of constantan,  $E_{Co}$  was the EMF between the constantan thermoelements (as corrected for the reading during the isothermal) and  $\gamma(\delta T)$  was the temperature drop between the constantan thermoelements where  $\gamma$  is a scale factor (near unity) determined during knife edge distance measurements. As shown in Table 5, the Seebeck of Mo determined in this fashion was uncertain by  $\pm 0.39 \mu\text{V}/\text{K}$  at 400 K and this greater error in  $S_{Mo}$  as determined using the constantan thermoelements as compared to the error using the Pt thermoelements has an interesting consequence which will be discussed later.

#### Indeterminate Errors

In addition to the above, there are some error sources which are not amenable to analysis and must be checked. For example, inhomogeneity in one of the Pt wires could cause a spurious thermal EMF which would not be corrected by determining the EMF under isothermal conditions. One way to test for hidden errors is to measure on similar samples and examine the results for consistency. This approach will test system reproducibility and precision; and if the samples are of different sizes, there are several error sources which may become apparent if they have been assessed incorrectly. These include uncertainties in specimen area and heat exchange between specimen and guard cylinder. Also, the Seebeck coefficient measurements are independent of sample size and  $S_{Mo}$  from the Pt and constantan thermoelements serve as good tests of measurement precision of the  $\delta T$ .

## RESULTS

Electrical Resistivity

Electrical resistivity data for the two specimens are shown versus T in Fig. 7 as percentage deviations from the arbitrary polynomial

$$\rho = 6858.18/T^2 - 156.952/T - 0.13238 + 0.018397 T + 6.289 \times 10^{-6} T^2 \quad (11)$$

where  $\rho$  is in  $\mu\Omega\text{-cm}$  and T in K. The data have not been corrected for thermal expansion but they have been corrected for the small residual resistivity values noted in Table 1. Near 80 K it would appear that  $\rho$  of the two specimens differ by 0.6%; but when these values were adjusted to the same temperature, the difference was only 0.32%. Above 120 K, the electrical resistivities deviate slowly about Eq. (11) and it can be seen that all values would be within a band of  $\pm 0.07\%$  with the exception of 2 points on specimen B near 297 and 301 K. All  $\rho$  values, with the exception of these two, were obtained using the Chromel-P wires of the specimen thermocouples and it may be that the high values of  $S_{\text{Mo-Co}}$  caused some error on these two data due to the Peltier effect since results from the Chromel-P wires gave 0.02% agreement with independent knife edge results. However, the  $\rho$  data from the two samples of Mo are well within the combined uncertainties of the measurements.

It is difficult to minimize all the uncertainties in  $\rho$  when tandem measurements of  $\lambda$  and S are desired. In general, accurate  $\lambda$  measurements dictate a large specimen  $\lambda A$  which causes some problems in  $\rho$  measurements due to the low voltage drops, especially at low T. The voltage drops down the specimen can be increased with larger currents; but it must be remembered that the larger current dictates larger input lead wires which must be thermally grounded to guard against heat leak.

### Seebeck Coefficient

The values of  $S_{Mo}$  as determined from the two specimens are shown versus  $T$  in Fig. 8 as deviations in  $\mu v/K$  from the empirical equation

$$S_{Mo} = 185.027/T - 5.15561 + 0.034522 T . \quad (12)$$

Representative data points have uncertainty bars included; and although the error using Pt wire is less than that using constantan, all data are well within the measurement uncertainty. The Seebeck coefficient is an extremely valuable system test when measurements of  $S$  are made with respect to two materials as is the case for specimen B.

This can be seen by first noting that  $S_{Mo}$  from Pt and  $S_{Mo}$  from constantan agree to within  $0.07 \mu v/K$  above 100 K for specimen B. An uncertainty of  $\pm 0.27\%$  has been claimed for the determination of the  $T$  difference between T.C. #3 and #4. If we assume, however, that  $\delta T$  were in error by 1% at 300 K, this would shift  $S_{Mo}$  (Pt) by  $0.1 \mu v/K$  and  $S_{Mo}$  (Co) by  $0.5 \mu v/K$  which would be a readily observable effect considering the precision of Fig. 8. Thus if the error in  $\delta T$  deviated above the claimed uncertainty,  $S_{Mo}$  (Pt) and  $S_{Mo}$  (Co) would diverge rapidly and provide a warning about the  $\lambda$  data.

### Thermal Conductivity Results

The measured  $\lambda$  of the two specimens have been corrected for the small residual impurity by assuming that impurity scattering is elastic and the lattice component of  $\lambda$  negligible so that

$$\lambda = \left\{ \frac{1}{\lambda_{meas}} - \frac{\rho_{4.2 K}}{2.443 \times 10^{-8} (v/K)^2 T} \right\}^{-1} \quad (13)$$

where the constant is the Sommerfeld value of the Lorenz function.<sup>(6)</sup> As was the case for the electrical resistivity, this correction was 0.1% at 80 K and 0.01% at 300 K. The  $\lambda$  results are for pure Mo uncorrected for thermal expansion.

Figure 9 presents the percentage deviations of the  $\lambda$  results from the arbitrary equation

$$\lambda = 1.0 \times 10^6/T^3 - 14043/T^2 + 88.957/T + 1.3115 - 1.7184 \times 10^{-4} T - 2.9005 \times 10^{-7} T^2 . \quad (14)$$

All data from this study are within a  $\pm 0.2\%$  band with the exception of one value from specimen A at 380 K, and most data are within a  $\pm 0.1\%$  band.

Each set of data appears precise to within  $\pm 0.1\%$  (with the one exception) and if we look at the error sources in  $\lambda$  which could lead to imprecision we see that  $\frac{\Delta(\delta T)}{\delta T}$  would contribute  $\pm 0.27\%$  and  $\frac{\Delta P_c}{P_c}$  would contribute  $\pm 0.07\%$  for a total of  $\pm 0.34\%$  possible on imprecision. Thus the agreement of the results from the two samples is within the combined errors and the imprecision is well within expectations.

In 1968, measurements were made on specimen A in the predecessor of the present device and these data have been corrected to the IPTS-68<sup>(23)</sup> and are also shown on the figure for comparison. Although the precision of the older data is inferior, the agreement is excellent considering the  $\pm 1.2\%$  most probable error claimed for the older set of data. This close agreement also substantiates the analysis for heat exchange through the insulation which indicated that the guard-specimen temperature mismatch would have a small effect on the measured  $\lambda$  of Mo. Values of  $\lambda$  from a recommended curve by Ho et al.<sup>(30)</sup> are also shown in Figure 9 for comparison to the present results. This recommended curve is within 1% of our values at 100 K and 400 K and has a maximum difference of 3.7% at 150 K.

## CONCLUSIONS

This technique represents a considerable improvement over its predecessor although all major changes did not necessarily represent improvements.

The connections for all wires on the flange within the chamber were at or near the cooling bath temperature at all times and this prevented small thermal EMFs at the connections from changing with time and invalidating the thermocouple calibrations against the PRT. In situ thermocouple calibrations with the PRT and the Guildline Potentiometer reduced the error in  $\delta T$  measurement from 1% to 0.27%. This led to major improvements in Seebeck coefficient and thermal conductivity determinations.

The copper section on the guard cylinder was a poor choice since an unfavorable temperature profile was established along the guard and this led to a larger specimen-guard mismatch than was obtained with a brass tube for the entire guard cylinder length. Calculations indicated that a maximum correction of 0.06% would be needed for specimen A because of this mismatch. Although this correction was quite small for Mo, it would be larger for materials of lower  $\lambda$ . For this reason, a better design would be a uniform guard cylinder for its entire length with a small Cu block attached for thermally grounding wires from  $H_1$ .

The technique is laborious and time consuming and patience must be exercised in attaining true thermal steady state which normally required about two hours. This is especially true for the in situ calibrations of the two specimen thermocouples against the PRT because of the thermal resistance between them. The technique is a factor of 4 slower than its predecessor and, for this reason, should only be used when a problem requires the increased precision and accuracy which the technique will deliver.

## ACKNOWLEDGEMENTS

We gratefully acknowledge T. G. Godfrey for his assistance with the heat exchange calculations, D. L. McElroy and T. G. Kollie for careful text review, and D. L. McElroy for the unpublished thermal conductivity data on the fibrous insulation.

## REFERENCES

1. M. J. Laubitz in Thermal Conductivity, Vol. 1, Chapter 3, ed. R. P. Tye, (Academic Press, London, 1969), p. 111.
2. J. P. Moore, R. S. Graves, and D. L. McElroy, C. J. Phys. 45, 3849 (1967).
3. J. P. Moore, W. Fulkerson, and D. L. McElroy, J. Am. Ceram. Soc. 53(2), 76 (1970).
4. J. P. Moore and R. S. Graves, J. Appl. Phys. 44(3), 1174 (1973).
5. M. J. Laubitz and D. L. McElroy, Metrologia 7, 1 (1971).
6. R. K. Williams and W. Fulkerson, Thermal Conductivity, Proceedings of the Eighth Conference, ed. C. Y. Ho and R. E. Taylor (Plenum Press, New York, 1968), pp. 389-456.
7. G. A. Slack, Phys. Rev. 122, 1451 (1961).
8. J. G. Cook, M. P. Van der Meer, and M. J. Laubitz, C. J. Physics 50(12), 1386-1401 (1972).
9. Carborundum Co., Fiberfrax, ceramic fiber packed loosely to a density of approximately  $0.025 \text{ g/cm}^3$ .
10. This separate experiment was carried out in a small radial system with a length to diameter ratio of about 6. The thermal conductivity of the insulation was  $7.1 \times 10^{-13} \text{ T}^3 \text{ (w/cm-deg)}$ .
11. Hewlett-Packard D.C. Power Supply, CCB Series Model 6181B, Ripple  $<0.04\%$ , stability better than  $\pm 0.01\%$ .
12. Leeds and Northrup Co., Cat. No. 4221-B, nominal resistance 0.1 ohm,  $\pm 0.001\%$ .
13. Guildline Instruments Ltd. Direct Current Comparator Potentiometer Type 9930, uncertainty on X0.1 range =  $\pm 0.0001\% + 0.01 \mu\text{v}$ , uncertainty on X0.01 range =  $\pm 0.0002\% + 0.005 \mu\text{v}$ .
14. Leeds and Northrup Co., Potentiometer Type K-5 (7555), uncertainty  $\pm 0.005\%$  of reading +  $0.1 \mu\text{v}$ .

15. Leeds and Northrup Co. Volt Box, Cat. No. 7593, uncertainty as calibrated less than  $\pm 0.01\%$ .
16. Astrodyne, Inc., Thermal-Bond 312, Burlington, Massachusetts.
17. Guildline Instruments Ltd. Low Thermal Selector Switches Type 9145A.
18. Guildline Instruments Ltd. SCW two conductor cable.
19. T. G. Godfrey, W. Fulkerson, T. G. Kollie, J. P. Moore, and D. L. McElroy, Oak Ridge National Laboratory, ORNL-3556 (June 1964), p. 7.
20. Leeds and Northrup Co., Cat. No. 4025-B, nominal resistance 10 ohms,  $\pm 0.0002\%$ .
21. Model S1059-1 (Serial No. 57) of Minco Products, Inc., 740 Washington Ave. N., Minneapolis, Minnesota.
22. W. V. Johnston and G. W. Lindberg, Rev. Sci. Instr. 39, 1925 (1968).
23. Metrologia, Vol. 5, #2, April 1969, pp. 35-44.
24. F. R. Caldwell, J. Res. Nat. Bur. Std. 69c(2), (April-June 1965).
25. T. G. Kollie, Oak Ridge National Laboratory, ORNL-TM-1187 (August 1965).
26. R. L. Powell, W. J. Hall, C. H. Hyink, L. L. Sparks, G. W. Burns, M. G. Scroger, and H. H. Plumb, N.B.S. Monograph 125, U. S. Department of Commerce, National Bureau of Standards, Washington, D.C. (1973).
27. J. P. Moore and R. S. Graves, from unpublished data obtained by comparison to lead (1973).
28. L. L. Sparks and R. L. Powell, "Final Report on Thermometry Project," N.B.S. Report 9249 (June 30, 1966).
29. W. D. Turner and M. Siman-Tov, "Heating 3-- An IBM 360 Heat Conduction Program," Oak Ridge National Laboratory, ORNL-TM-3208 (February 1971).
30. C. Y. Ho, R. W. Powell, and P. E. Liley, "Thermal Conductivity of Selected Materials - Part 2," NSRDS-NBS 16 (February 1968).

## LIST OF FIGURES

Fig. 1. Guarded-longitudinal-heat flow apparatus showing position of PRT and relative positions of specimen thermocouples and Pt wire. All wire junctions are similar to the one shown.

Fig. 2. Circuitry pertinent to the thermal conductivity technique with the resistivity circuit omitted for clarity.

Fig. 3. Detail of PRT attachment to heater base.

Fig. 4. Detail of the thermal grounding procedure for wires coming from  $H_1$ .

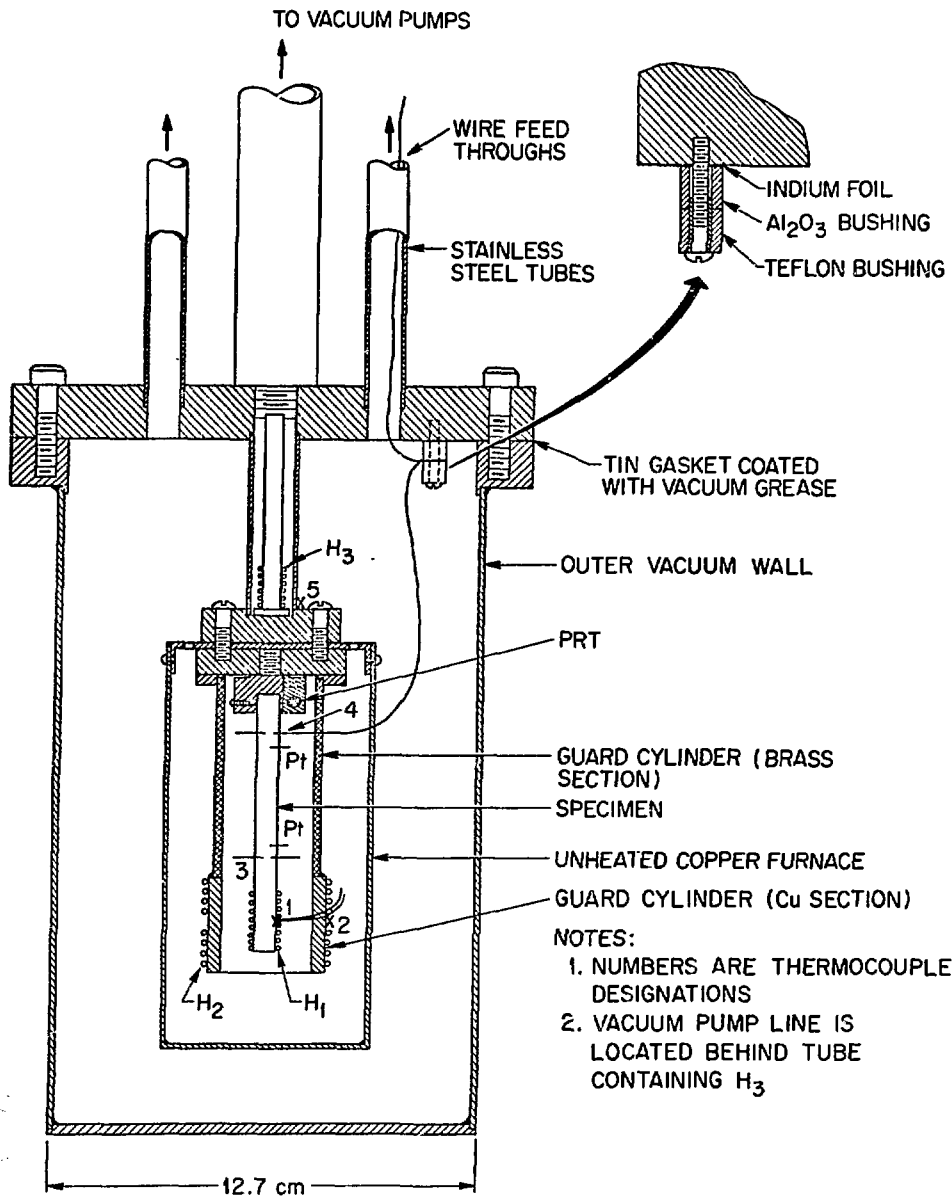
Fig. 5. Geometry and dimensions used for calculation of temperature distributions for specimen A.

Fig. 6. Temperature profiles of inside guard wall and specimen surface versus  $z$  for the case of a Cu section on the guard and for a guard cylinder of brass over the entire length.

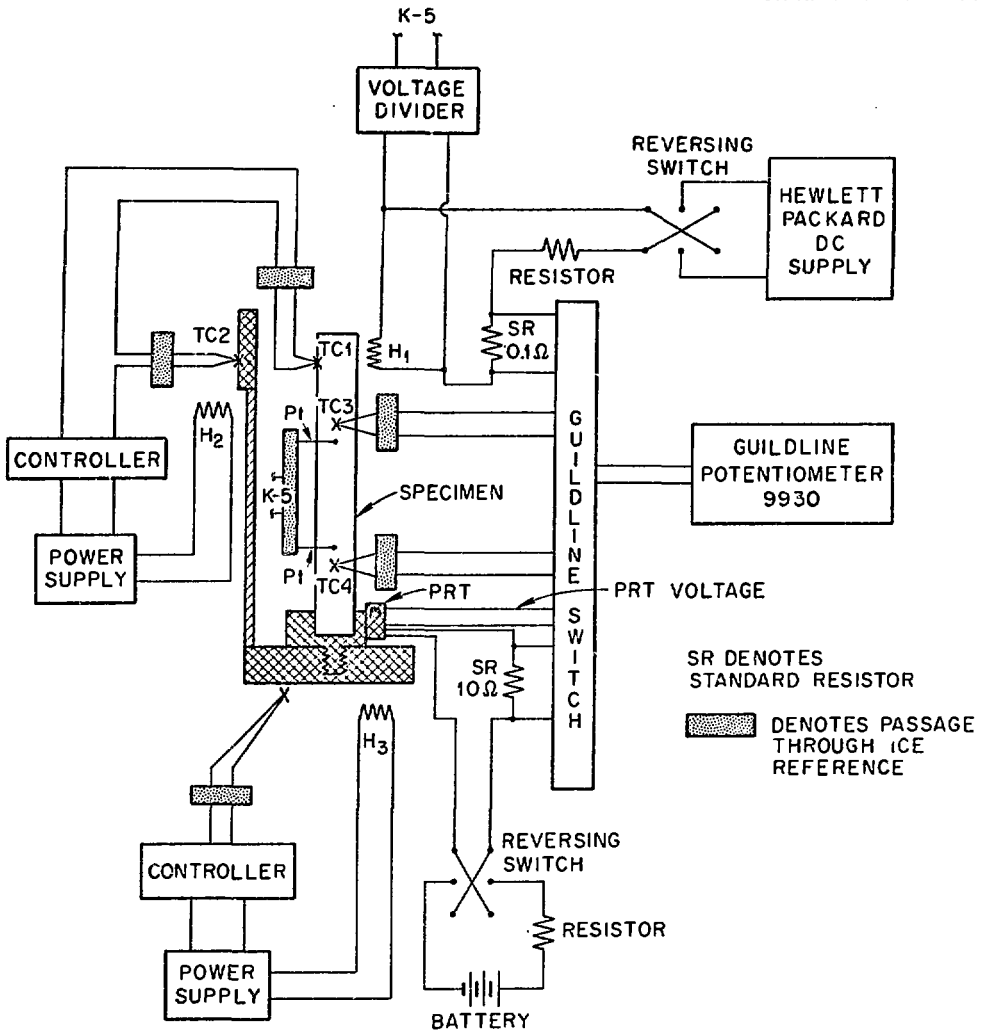
Fig. 7. Percentage deviation of the measured  $\rho$  data from an arbitrary equation  $[(\rho_{\text{meas}} - \rho_{\text{EQ}}) \times 100 / \rho_{\text{EQ}}]$  versus temperature.

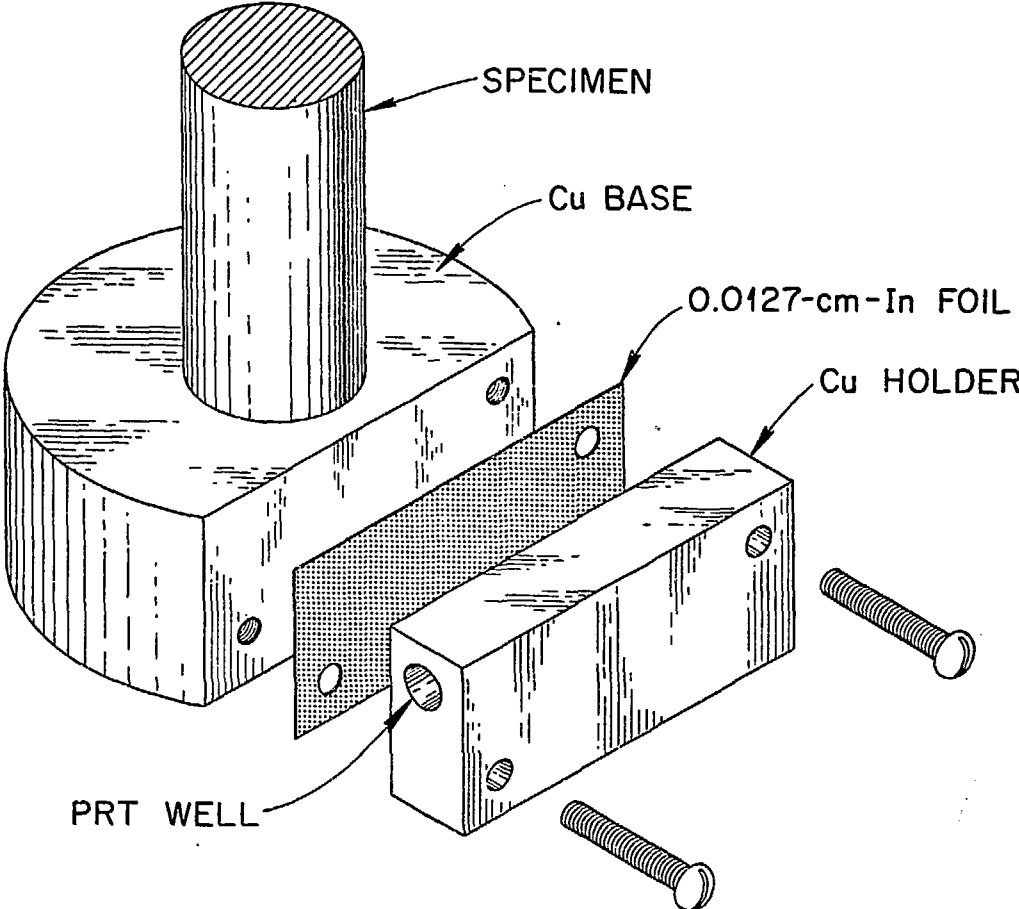
Fig. 8. Deviation of the measured  $S_{\text{Mo}}$  data from an arbitrary equation  $[S_{\text{Mo}}(\text{meas}) - S_{\text{Mo}}(\text{EQ})]$  versus  $T$ . Data for specimen A was obtained using constantan and data for specimen B was obtained with both Pt and constantan.

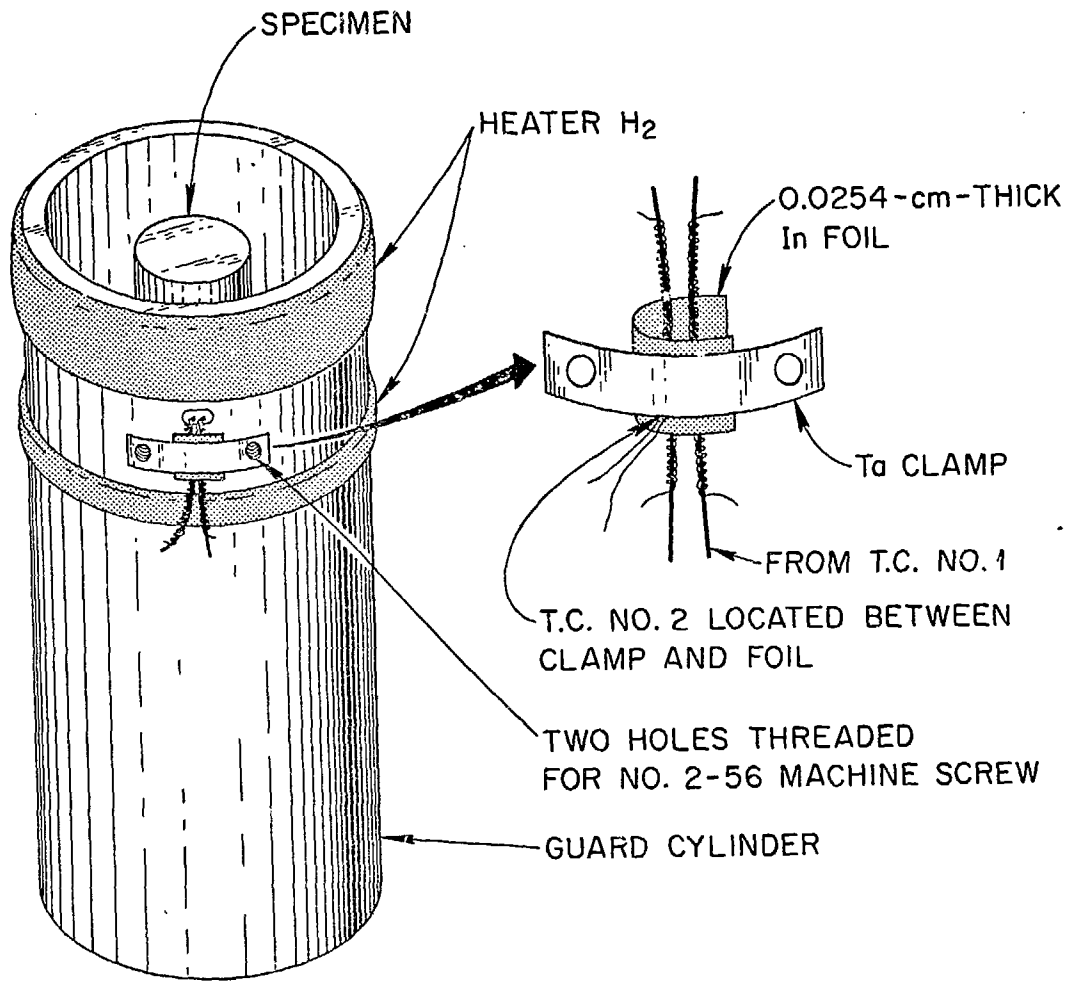
Fig. 9. Percentage deviation of measured  $\lambda$  data from an arbitrary equation  $[(\lambda_{\text{meas}} - \lambda_{\text{EQ}}) \times 100 / \lambda_{\text{EQ}}]$  versus  $T$  for specimen A and B. Previous data from specimen A are also shown for comparison.

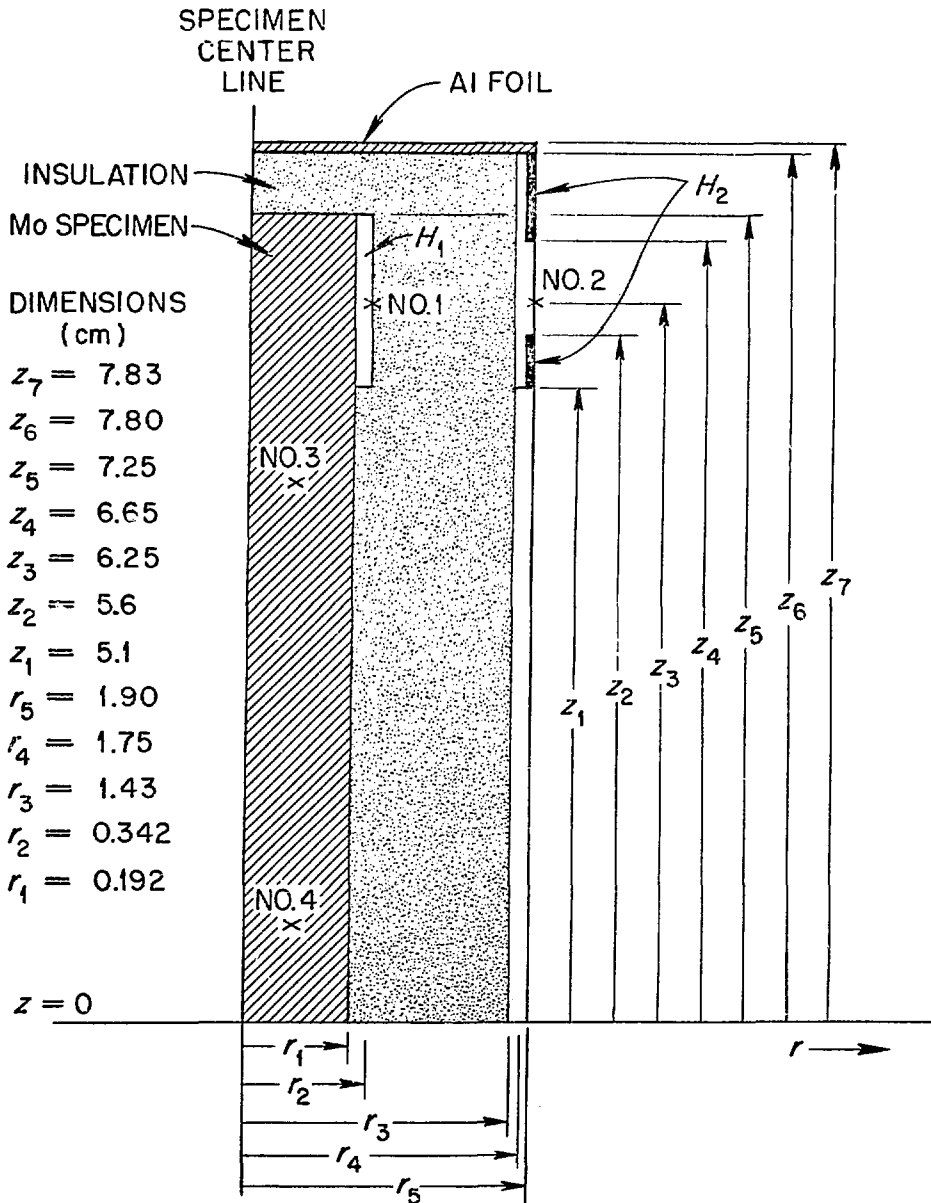


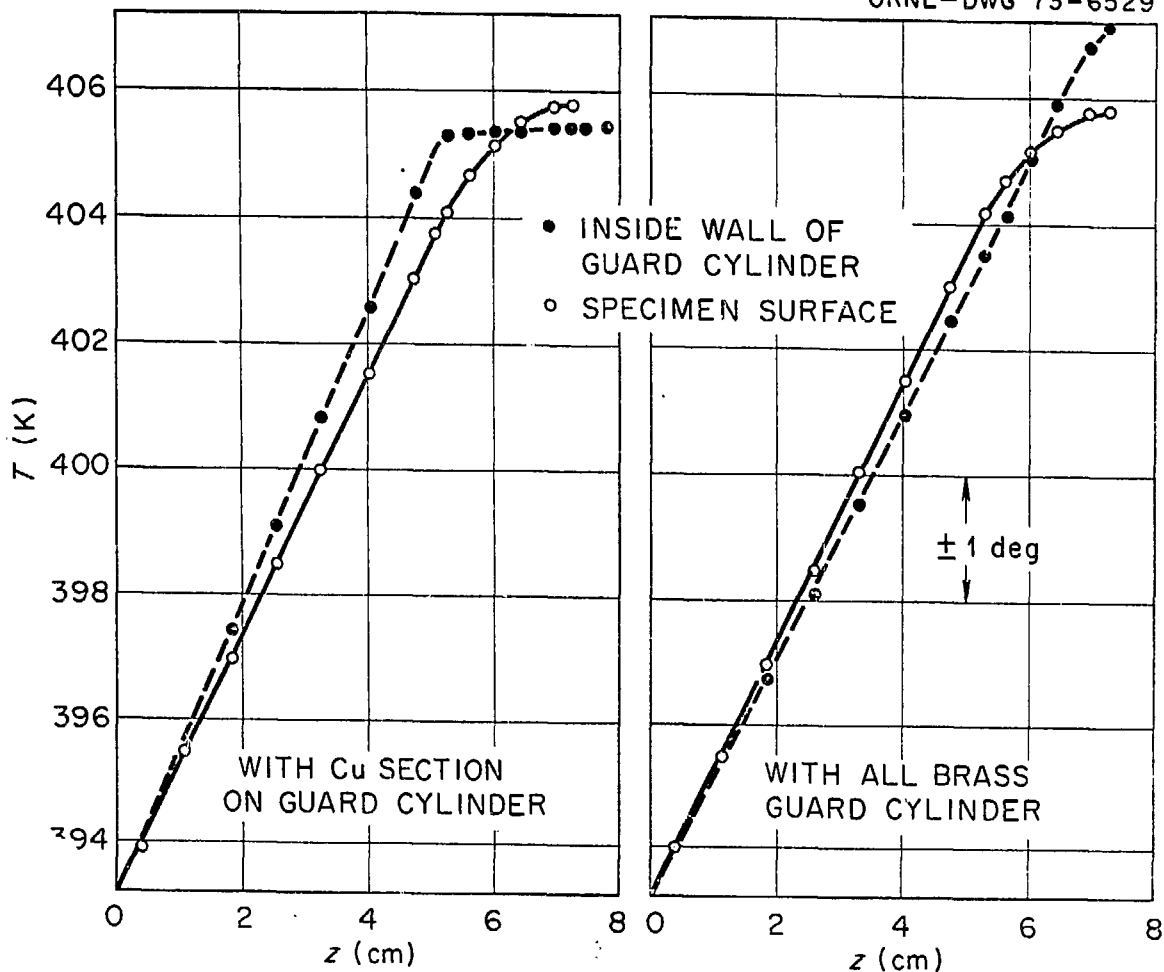
- NOTES:
1. NUMBERS ARE THERMOCOUPLE DESIGNATIONS
  2. VACUUM PUMP LINE IS LOCATED BEHIND TUBE CONTAINING H<sub>3</sub>











ORNL-DWG 73-6531

